CONF-8609133

GA Technologies

MASTER

GA-A18591

HTGR FUEL ELEMENT STRUCTURAL DESIGN CONSIDERATIONS

GA-A--18591

DE86 016096

by

R. ALLOWAY, W. GORHOLT, F. HO,
R. VOLLMAN, and H. YU

This is a preprint of a paper to be presented at the IAEA Specialists' Meeting on Graphite Component Structural Design, September 8-11, 1986, Japan Atomic Energy Institute, Japan.

Work supported by
Department of Energy
Contract DE-AC03-84SF11962

GA PROJECT 7700
SEPTEMBER 1986

EAB

DISCLAIMER

DISCLAIMER

HTGR FUEL ELEMENT STRUCTURAL DESIGN CONSIDERATIONS

R. Alloway, W. Gorholt, F. Ho, R. Vollman, H. Yu
GA Technologies Inc.

ABSTRACT

The structural design of the large HTGR prismatic core fuel elements involve the interaction of four engineering disciplines: nuclear physics, thermo-hydraulics, structural and material science. Fuel element stress analysis techniques and the development of structural criteria are discussed in the context of an overview of the entire design process. The core of the proposed 2240 MW(t) HTGR is described as an example where the design process was used. Probabalistic stress analysis techniques coupled with probabalistic risk analysis (PRA) to develop structural criteria to account for uncertainty are described. The PRA provides a means for ensuring that the proposed structural criteria are consistant with plant investment and safety risk goals. The evaluation of cracked fuel elements removed from the Fort St. Vrain reactor in the U.S.A. is discussed in the context of stress analysis uncertainty and structural criteria development.

ACKNOWLEDGEMENTS

The authors would like to thank Mr. A. Millunzi, Acting Director, Division of HTGR, U.S. Department of Energy, for approval to publish this paper. Thanks are also expressed to the management of GA Technologies Inc. for permission to write and present this work, which was supported by the Department of Energy, San Francisco Operations Office Contract DE-AC03-84SF11962.

Introduction

The design of the replaceable graphite fuel elements and the development of structural criteria for the replaceable graphite fuel elements in the high temperature gas cooled nuclear reactor (HTGR) developed within the National Gas Cooled Reactor Program in the U.S.A. are the subjects of this article. Probabilistic Risk Assessment (PRA) techniques are used to tie the fuel element structural design to national safety goals. The consequences of damaged graphite components is included in the criteria. Fuel elements cracked in service at the Fort St. Vrain HTGR in Colorado are discussed in this context.

Design Description

The U.S. HTGR is a prismatic block design with fuel pins and coolant holes in a triangular patterned array throughout the graphite moderator. Primary coolant (helium) flows downward during normal power production. To facilitate refueling, the moderator mass is made up of identically sized hexagonal graphite elements about 36 cm across flats and 79 cm long stacked in columns on a core support floor. Gaps between fuel elements are sized to facilitate refueling. The core of the previously proposed 2240 MW(t) HTGR is described as an example of a typical design as shown in Figure 1.

There are two types of fuel elements in the core, 1) fuel elements with a regular array of fuel pins and coolant holes, and 2) control elements with the regular array of fuel pins and coolant holes disrupted by large vertical holes for inserting control rods or reserve shutdown material into the core. The elements are shown in Fig. 2. There are also hexagonal reflector elements surrounding the active core which have no fuel pins, but are not the subject of this article. The fuel elements residence time in the core is about four years.

Design Approach

The structural design of an HTGR core involves the interaction of four engineering disciplines: nuclear physics, thermo-hydraulics, structural mechanics, and material behavior. The structural design must have sufficient margin against failures to meet the overall objective of producing safe and ecomonic power. This overall objective is separated into several goals which have a large impact on the structural design. Three of these goals are to produce a design which will 1) maintain safe plant operation, 2) maintain plant protection, and 3) maintain control of radio nuclide release to the public as shown diagramitically in Fig. 3.

Maintaining safe plant operation involves a sufficiently conservative design to ensure that normal operation within scheduled and planned events is assured. Maintaining plant protection requires that the design is sufficiently conservative to keep the risk to the investment in the plant from unscheduled events which could jeopardize its economic basis to an acceptable value. Maintaining control of radionuclide release to the public requires that it be shown that the system and structural performance is adequate to limit the risk to the health and safety of the public to acceptible levels and meet national safety goals.

Analytical Approach

The design of an HTGR core is an iterative process involving 1) nuclear analysis to determine core flux/fluence time histories, power density, fuel burnup, and refueling schemes, 2) thermal hydraulic analysis to determine primary coolant flow rates and distribution within the core, and fuel and moderator temperatures, 3) stress analysis for thermal/irradiation conditions and mechanical loads to assess structural adequacy. This process and some of the important aspects are illustrated in Fig. 4.

The detailed analysis involves many computer codes to generate the loads and boundary conditions for input to the stress analysis code. This series of analyses is shown in Figure 5 where the name and function of some of the codes is indicated.

Loads and Thermal/Irradiation Conditions

Mechanical loads are caused by the core pressure drop, deadweight, live loads, such as equipment weights, flow induced vibration, acoustic vibration, and earthquakes. Seismic loads are the most important of these and are derived by dynamic analysis using dynamic codes.

Thermal conditions imposed on the fuel elements come from the primary coolant temperature, pressure, and flow rate. In addition, the fuel elements are heated by fuel pin heat production and heating caused by gamma capture in the graphite.

Nuclear conditions important to the stress analysis are power and neutron flux distribution time history. The neutron fluence time history is needed to determine the effect of radiation on material properties. These inputs are obtained from the core nuclear physics analysis.

Effects of Operating Environment

The thermal/nuclear environment within the core plays a major role in the fuel element design.

The neutron fluence causes changes in the dimensions, creep rate, stress-strain behavior, strength, thermal conductivity, and thermal expansion of the fuel element block graphite. Graphite properties also change with temperature. These changes are accounted for in the design and analysis.

Fluence and temperature cause dimensional change and strain within the fuel element. The stress free change in dimensions are used to predict the gap size between elements during operation. In addition, the dimensional change gradient due to neutron fluence and temperature distribution are used to calculate the irradiation and thermal strains and any change in gaps due to fuel element distortion. The resulting time dependent gap changes effect primary coolant flow distribution, predicted temperatures, and ultimately thermal-irradiation induced stress. The block responds by deforming to come into equilibrium with the internal stress field. The irradiation induced creep strain will cause stresses to relax during operation. These are called operational stresses. Upon removal of the temperature and radiation flux during shutdown the block responds to the permanent creep strain and removal of thermal strain by coming into equilibrium with a residual internal stress field called the shutdown stresses.

Stress Analysis

A survey of all the fuel and control elements is conducted using a simplified thermal and stress analysis method to determine the location of highest to the lowest stressed elements caused by the radiation and thermal environment. A visco-elastic material model is used to account for environmental effects. From this and judgment based on experience elements are chosen for detailed stress analysis.

The time dependent thermal analysis is conducted on the selected elements using a finite element code which calculates the temperature field in the fuel element using a plenum to plenum fluid flow/heat balance over the entire length of the fuel column and boundary conditions from a core wide thermal-hydraulic analysis.

The time dependent thermal/irradiation induced stress field is calculated using a finite element code utilizing the generalized plane strain 8-node quadrilateral element. A plane normal to the axis of coolant and fuel pin holes can be modeled quite accurately with this code. A finite element mesh is shown in Figure 6 for a standard fuel and control element.

The graphite material behavior is modeled as visco-elastic using a combined Maxwell-Kelvin model to account for both transient and steady state creep. The effect of fluence and temperature is accounted for in the other material properties. Mean values of properties are used throughout the analysis.

The spatial and time (fluence) variation in mean strength within a fuel element is considered when comparing stress to strength at a particular point. Stress-to-strength ratios are used to account for the spacial variation in strength because stress relative to the strength at a point is important, not just the maximum stress. For example, it is possible that the maximum stress occurs at a location of high strength making it less critical than a lower stress occuring at a point of low strength. Thus, the maximum fraction of stress to strength is a more realistic measure of the potential for failure at a point in the fuel element than the maximum stress alone. The mean strength distribution is shown in Figure 7 for the axial direction and in the r-θ plane. Note that the maximum strength is in the axial direction on the outside middle of the block. The block is weakest in the r-θ plane in the middle of the block.

Typical results of the thermal analysis are shown in Figure 8. The global temperature distribution is shown in Figure 8(a) showing the block to be fairly uniform in temperature except for a hot spot near the middle and colds spots at each outer corner of the hexagonal element. Note the steep local temperature profiles between coolant holes and from fuel pins to coolant holes along the symmetry line in Figure 8(b). This difference in global/local temperature distribution is an indication that much of the thermal stress is induced by local thermal gradients. Irradiation induced stress tends to be caused by global differences in irradiation shrinkage across the fuel element.

Results of the stress analysis indicate that the fuel element is generally in compression in the center and tension in the peripheral portion as shown in Figure 9(a). The maximum tensile stress occurs at the cold spots (corners of the hexagon). The local stress along the symmetry line changes dramatically between coolant and fuel holes with the stresses in the r-θ plane generally higher than in the axial (Z) direction. The maximum stress to strength ratio (in the r-θ plane) time history is shown in Figure 10. The maximum operating stress generally occurs in about one year while the maximum shutdown stress always occurs at end of fuel element life (4 years). From the stress analysis results it is found that the highest thermal/irradiation induced in-plane stress to strength ratio is about 50% higher than the highest axial (out of plane) stress to strength ratio.

Stress produced by mechanical loads such as seismic are calculated using a linear elastic material model. These stresses are combined with the thermal/irradiation induced stress by superposition because of the short time duration of the seismic event. Stress to strength ratios are calculated for the combined stress fields to determine the location of highest stress to strength ratio.

Fuel Element Damage

Damage to fuel elements could occur by cracks initiated at the location of the highest stress to strength ratio. There are two basic kinds of cracking, 1) web cracking between holes with crack surfaces parallel to the axes of holes, and 2) across block cracking with the plane of the crack perpendicular to the axis of the holes. Web cracking would be from hole-to-hole relieving the in-plane stress field with the holes acting as crack arresters. Across block cracking would not have the same crack arresting geometric feature but cracks would tend to propogate into a decaying stress field. It is apparent that across block cracking has a greater safety consequence since a control element cracked in this way would tend to inhibit control rod and reserve shutdown material insertion. Across block cracking in the fuel element would be of less concern since it would tend to disrupt the alignment of coolant passages, but still allow some flow of coolant. A small number of blocks cracked in this manner would be tolerable to the extent that investment and safe shutdown risk is acceptable.

Crack progression studies (web cracking) are conducted by assuming that the highest stressed web relative to local strength completely cracks resulting in the redistribution of the stress field within the element. Then, the next highest stressed web cracks of the remainder, and so on. These predicted web stresses are usually well below the strength. Thus, it is more proper to think of the highest stressed web as having the highest probability of cracking relative to the other webs. The same analysis method discussed above is used to assess the progression of cracks in fuel elements.

The finite element model is modified in a progressive way to account for the loss of continuity across the crack. Assuming that quality control procedures in the manufacture of the fuel elements eliminates blocks with large disparate flaws (cracks), web cracking would occur before across block cracking due to the generally higher inplane than axial stress to strength ratios. The results show that by the first web cracking the stresses in the block drop dramatically except in the webs adjacent to the cracked web. The adjacent web inplane stress rises sharply causing probable failure of the second web. The third web has a high stress too and may crack. However, after the third web cracks the internal forces are so relaxed that even local stress is low tending to arrest further cracking.

These cracking patterns have an inconsequential effect on fuel block performance. There is an insignificant perterbation on coolant flow, fuel rods are uneffected since they are still contained in their holes, and seismic loads applied in the right direction tend to open these cracks but if the next web cracks, it propagates into another hole. In addition this type cracking does not effect fuel block removal unless complete fracture of the block into the two pieces occurs. The arresting nature of these cracks indicates low probability of a block fracturing into two pieces.

Two such cracked blocks were retrieved from the Fort. St. Vrain HTGR in Colorado. These blocks were located one over another at the outer periphery of a refueling region which had been experiencing a high flux gradient due to control rod insertion as shown in Figure 11. The cracked blocks were routinely removed with the fuel handling machine without incident. Subsequent physical examination of the cracked blocks showed that the crack extended from top to bottom of the block, was tight, and did not appear to have effected coolant flow in the hole. At the top and bottom (about 6 cm from each end) adjacent webs were cracked locally indicating the onset of the type of crack progression previously described. No other cracks were found.

An extensive crack progression analysis of the type described above was conducted on the FSV fuel elements to develop an understanding of what caused these cracks. The actual operating history of the plant was used to develop the flux, power distribution, flow rate, and temperature in the fuel element. Expected gaps around the fuel column and flow through them were used. The stress to strength ratio calculated for nominal conditions was 0.7 and was located at a point in the cracked web as shown in Figure 12. A parametric study where gap size and flow were varied revealed that had the gap on the outside of the fuel column been four times nominal the added cooling effect would increase the stress beyond the mean strength which would crack the block 50% of the time. In addition, when the first web cracked the maximum stress in the adjacent web increased beyond the strength as shown in Figure 13. The analysis predicted that two webs would have cracked and possibly a third. Crack arrest was predicted after the third web cracked. Inspection of the block showed that the second web was cracked only at the top and bottom of the block and that the third web had evidence of crack initiation. Thus, the analysis was somewhat conservative in predicting crack progression. The fuel elements all around the cracked blocks were analyzed and found to have stresses too low to expect cracking.

It is this kind of consequence analysis which helps keep in perspective the extent of failure needed to cause an investment risk or a safety concern. The failure of control rod elements has a greater consequence on safety because of control rod insertion requirements. This greater consequence when propagated through a PRA could result in a lower allowable stress to strength ratio than would be required for a standard fuel element to achieve an acceptable investment and safety risk.

Structural Criteria

Earlier structural criteria for fuel elements were developed using deterministic techniques completely. Prediction of nominal stress using "nominal" loads and material properties was used. This is similar to using statistical mean values. The concept of minimum strength was used where the lower bound of strength data was defined as the 99% probability of survival at a confidence level of 95%. Allowable stress to minimum strength ratios were assigned largely based on judgment and experience. Crack initiation was not allowed. These type limits were used to design graphite fuel elements in predecessors to the 2240 MW(t) reactor and are shown in Table 1(a). The traditional categories of Normal, Upset, Emergency, and Faulted conditions were used to separate power production design conditions from accidents. The consequence of analysis was considered in that during accidents damage to fuel elements was allowed if it could be shown that there was no interference with safe shutdown of the reactor and radionuclide release was acceptable.

Present stress limits are shown in Table 1(b). They are also deterministic when used in design analysis. However, they are based on the use of probabilistic stress analysis to statistically quantify the uncertainty in predicted mean stress. The statistically determined mean strength is also used. In the present criteria mean stress to mean strength ratios are used as stress limits to account for the spacial variation of strength within a single piece of graphite. These allowable ratios are developed by using PRA analysis techniques as a means to determine that the chosen allowable stress ratios will ensure that the plant investment and safety risk goals are met.

The consequence of failure is incorporated into the basis for the allowable stress ratios assigning different ratios to fuel, and control elements. In addition, within a given element, there are multiple allowables reflecting the tolerance of the nuclear core as a whole to a larger amount and higher probability of damage in a small group of elements (group 1), lessor and lower probability of damage in a larger group (group 2), and a very low probability of damage in the rest (group 3). The allowable stress ratios are also different for each type of stress state reflecting either investment risk or safety risk as limiting. The first three columns in Table 1(b) would be based on investment risk with seismic being the traditional operating basis earthquake (OBE). Note also that the less severe consequence of an unscheduled event during shutdown, when all control rods are inserted, would result in higher allowable stress ratios than during power production when control rods are generally withdrawn.

The choice of structural acceptance criteria is dependent on the accuracy of predicted stresses (i.e., methods with large uncertainty in accuracy require large margins in acceptance criteria and visa-versa.) Uncertainties in input loads and conditons, material behavior models, nuclear physics and thermal/stress analysis techniques propagate through the analysis giving commensurate uncertainty in predicted fuel element stress. A similar uncertainty will be inherent in the failure stress model chosen and the scatter in failure stress data. This familiar triad of stress prediction and failure uncertainty is shown in Fig. 14.

Performing a probabilistic stress analysis and a PRA is a way to evaluate how well the design of a plant and its various components achieve the goals and meet the risk limits of the plant. It also helps identify those aspects of the design and consequence of failure which contribute the most uncertainty to meeting performance and safety requirements. In this way one can focus effort on those identified critical aspects of the component design. For instance, the uncertainty in the value of a particular material property may dominate the uncertainty in predicted fuel element stress causing modification of the design or incorporation of a large margin against damage.

The stress uncertainty analysis is conducted by determining the probability density function and its cumulative distribution function, the coefficient of variation, skewness, and peakedness for each parameter in the analysis chain from prediction of fluences to gap sizes to fuel element stress to failure stress. Table 2 lists the parameters evaluated. Note the high uncertainty of interelement gap size and creep. Table 3 is a list of the stress prediction statistical parameters. Here, the end of life axial stress is the most uncertain.

The functional uncertainty distribution is determined by combining the various parameters uncertainty distribution functions using the random sampling Monte-Carlo simulation technique.

The results of such an analysis are shown in Table 4. Clearly the greatest uncertainty in the stress analysis results is contributed by the irradiation creep model and data, and the size of the gap between fuel elements. Gap size has a significant effect on local temperature distribution. Gap size uncertainty can be partially reduced by incorporating a design feature into the core which will control gaps caused by fuel column dimensional change and movements. The uncertainty due to irradiation dimensional change would be more difficult to reduce. Likewise, the creep model uncertainty will be difficult to reduce unless very carefully controlled, highly instrumented (and expensive) creep experiments are conducted.

The advantage of this approach is that it focuses attention on the parameters contributing the most to uncertainty and causing the greatest reduction in fuel element allowable stress-to-strength ratios. It allows research and design efforts to be prioritized effectively so that major problems can be identified and solved early in the design process.

A PRA is used to evaluate the risk of operating the plant. The risk is determined as the product of the frequency or probability per year of damage and the consequence of that type damage. The probability of damage is the area under a probability density function curve produced by the product of the probability density function of predicted stress and the cumulative probability function of strength as shown in Fig. 15. The probability density function of every important parameter or condition in the stress analysis and the strength probability distribution function are used in the analysis. The contribution of the reactor core risk to the total plant risk is determined.

If the probability is below the acceptance limit, then the allowable mean stress to mean strength ratio can be determined by arbitrarily shifting the predicted stress probability density function upward in stress (see Fig. 15) until the probability of damage is at the limit determined by the PRA (large shaded pdf in Fig. 15). The ratio of mean stress to mean strength for the shifted probability density function can then be used as the allowable stress ratio in other stress analyses provided the same techniques, material models, and input uncertainty are used. Additional margin can be incorporated at this point in the evaluation if desired. The PRA couples the probability of fuel element damage to the consequence of that damage and the risk goals so that arbitrarily conservative criteria are avoided. For example, if many fuel elements must be damaged before a contribution to safety risk is observed, why adopt a criteria which prohibits any damage?

Allowable stresses established in this way which reflect the number of damaged fuel elements, eliminate unnecessary conservatism in the design. For example, an unnecessarily conservative allowable stress criteria could cause the power density in the core to be set unnecessarily low resulting in an economic penalty in the design.

In summary, using the above techniques, structural criteria for replaceable graphite components can be developed which account for the differences in function, stress direction, and consequence to establish the proper stress limit for each case. A comparison of the deterministic stress limits used to design the core graphite components in earlier reactor designs and the probabilistic based allowables of the 2240 MW(t) reactor illustrate this (Table 1). The old criteria embraces the concept of "minimum strength" and maximum stress" and attempts to preclude crack initiation. Allowable stress ratios are set for the traditional load cases (i.e., normal, upset, emerging and faulted.) The 2240 MW(t) allowable stress ratios reflect the use of mean strength, mean predicted stress, the uncertainty in them, and the overall investment and safety risk goals. The consequence of failure is also accounted for in allowing a small percentage of the core elements to have high stress (low consequence of damage) while keeping the bulk of the elements at a lower stress to preclude damage which has an investment or safety risk.

During the preliminary design phase of the reactor several iterations of this analytical approach can be made to reflect improvements in experimental data, analysis, and design uncertainty until a set of allowable stress-to-strength ratios is established. The design can then be completed using these final allowable stress-to-strength ratios, with the analytical methods used in the process to predict mean stresses in the traditional deterministic way without further probabilistic stress analyses, Monte-Carlo simulations, and PRA.

Conclusions

Stress analysis and structural criteria for HTGR fuel elements developed in this way is a rational, logical, and provides a sound basis for licensing the reactor and reducing investment risk to the utility purchasing the plant.

TABLE 1

Earlier and Present Stress to Strength Limits

(a) Earlier Limits

Design Condition	Ratio of Norm Stress to Min. Strength
Normal Condition	0.7
Upset Condition	0.7
Emergency Condition	0.8
Faulted Condition	0.9

(b) Present Limits

Element Type	Ratio of Mean Stress to Mean Strength			
	Power Production	Shutdown	Seismic	Accidents
Std. Fuel Element				
Stress Group 1	0.35	*	*	*
Stress Group 2	0.31	*	*	*
Stress Group 3	0.26	*	*	*
Control Fuel Element	*	*	*	*
Replaceable Reflector Element	*	*	*	*

* These stress to strength ratios are being developed.

TABLE 2

Fuel Element Stress Analysis

Input Parameters and Their Uncertainty Distributions

Parameter	Distribution Type	Cov in %
Inter-Element Gap	Lognormal	39.3
Poissons Ratio	Lognormal	23.0
Steady State Creep Mobility, M^S	Weibull	22.0
Transient Creep Mobility, M^T	Weibull	22.0
Transient Creep Modulus, E^T	Weibull	22.0
Irradiation Strain	Normal	10.0
Thermal Conductivity	Normal	10.0
Elastic Modulus, E	Normal	9.2
Thermal Expancivity	Normal	7.9
Axial Power Factor	Normal	6.2
Column Power Factor	Normal	6.2
Core Presssure Differential	Normal	5.0
Inlet Coolant Temperature	Normal	5.0
Neutron Fluence	Normal	3.0

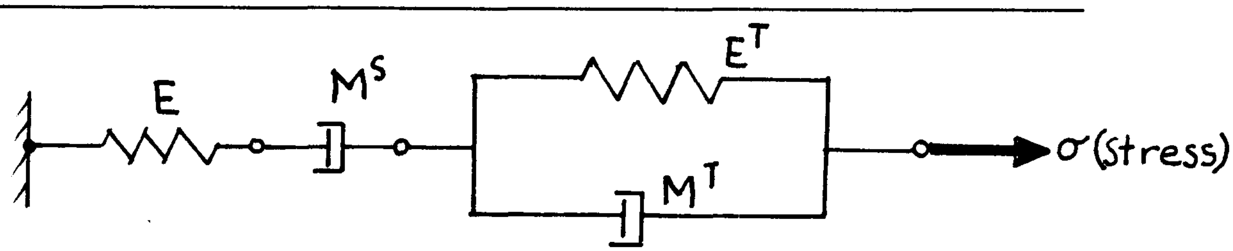

Maxwell-Kelvin Creep Model

TABLE 3

Uncertainty in Predicted Fuel Element Stress at
Various Plant Operating Conditons as Depicted
by Parameters of the Probability Distribution Function

Stress at Operating Conditon	Coefficient of Variation in %	Skewness	Peakedness
Axial end of life operating stress	47.7	1.85	5.33
Radial end of life operating stress	27.7	1.76	8.44
Axial end of life shutdown stress	27.3	0.54	3.43
Axial peak operating stress	24.4	1.26	4.47
Radial peak operating stress	21.7	1.00	4.03
Radial end of life shutdown stress	20.6	0.22	3.25

TABLE 4

Results of Fuel Element Stress Perterbation Analysis

Parameter	Parameter COV	Axial S/S Change %			Radial S/S Change %		
		Peak, OP	EOL, OP	EOL, SD	Peak, OP	EOL, OP	EOL, SD
Steady state creep, nom	-82.5	+74.5	+ 67.0	+27.5	+53.7	+ 20.6	- 0.84
+17.4% heat	-82.5	+74.2	+ 81.7	+43.7	+56.9	+ 59.7	+20.4
-17.4% heat	-82.5	+74.6	+163.4	-14.2	+52.6	+125.2	-29.9
Gap size	+66.	-10.5	+ 7.12	+14.8	-12.9	- 3.21	+19.9
	-66.	+ 7.95	+ 34.6	-24.9	+ 9.67	+ 20.9	-21.2
Transient creep modulus	30.	+ 5.1	+ 7.8	+ 3.1	+ 6.6	+ 5.0	+ 1.5
Poisson's ratio	+23.	+ 0.81	+ 1.33	+ 2.46	+ 1.39	+ 0.89	+ 2.43
Thermal conductivity, nom	+20.	-10.5	- 12.0	- 8.67	-10.9	- 13.4	- 8.67
, nom	-20.	+14.6	+ 19.4	+13.2	+15.4	+ 20.4	+13.1
Heat generation rate	+17.4	- 9.26	+ 85.9	+41.9	- 7.92	+ 44.8	+32.0
	-17.4	- 1.01	- 13.1	-35.3	- 1.72	- 10.8	-24.5
Irradiation strain	+ 7.2	+ 3.97	+ 6.54	+ 2.66	+ 4.13	+ 5.68	+ 1.69
Axial elastic modules	+ 6.3	+ 4.31	+ 3.01	+ 4.49	- 1.16	- 1.66	- 0.05
Radial elastic modulus	+ 6.3	+ 2.02	+ 2.90	+ 1.62	+ 7.53	- 6.88	- 6.33
Radial thermal expansivity	+ 5.4	+ 0.47	- 0.17	+ 0.27	+ 1.65	- 0.16	+ 3.86
Axial thermal expansivity	+ 5.	+ 1.42	- 0.41	+ 2.46	+ 0.462	- 0.31	+ 0.30
Coolant temperature	$-50^{o}F$	+ 8.84	- 5.64	-14.1	+24.5	-20.7	-13.2
	$+100^{o}F$	-17.2	+ 71.7	+29.1	-14.3	+32.5	+19.1

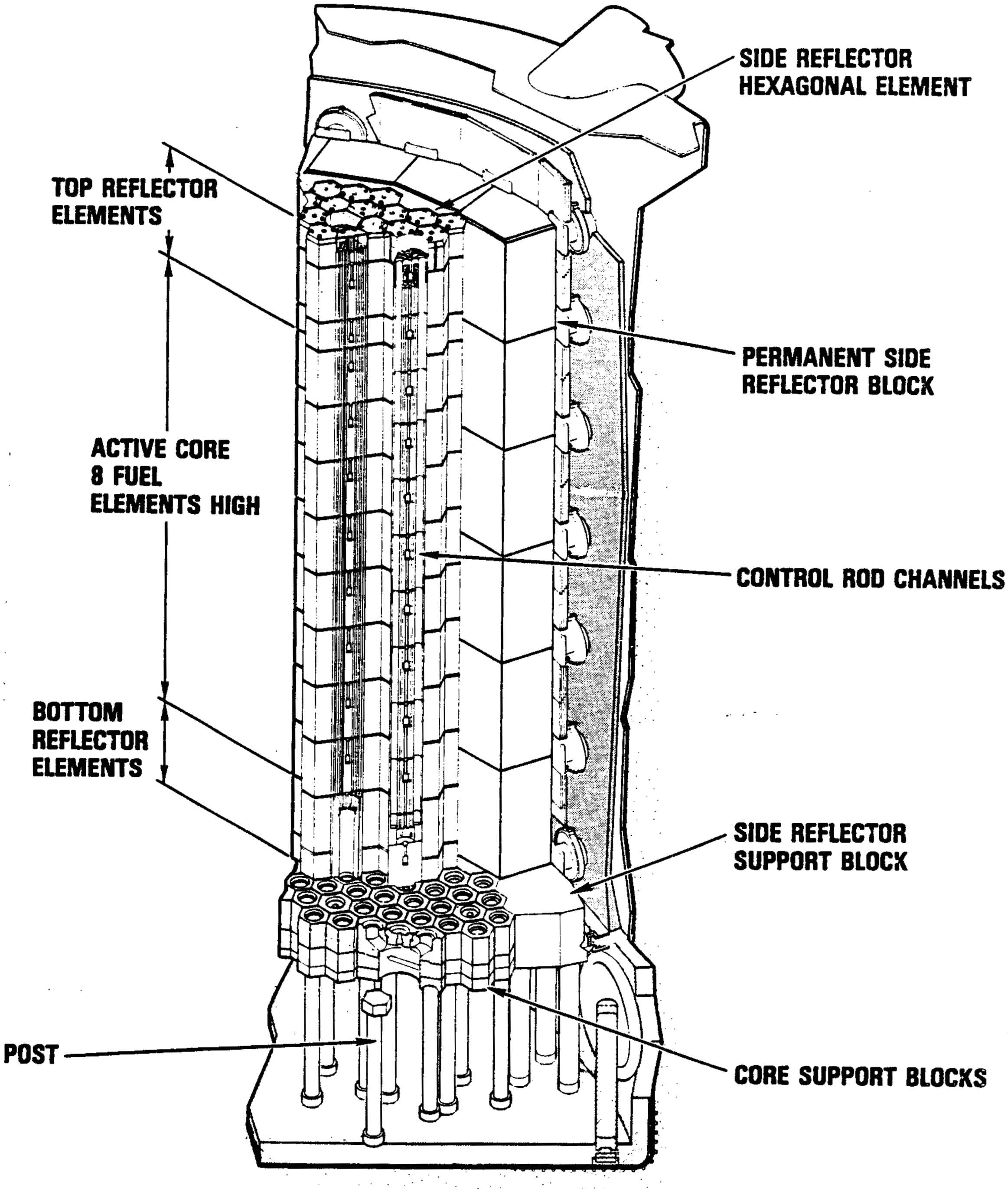

Fig. 1

PRISMATIC CORE CONFIGURATION

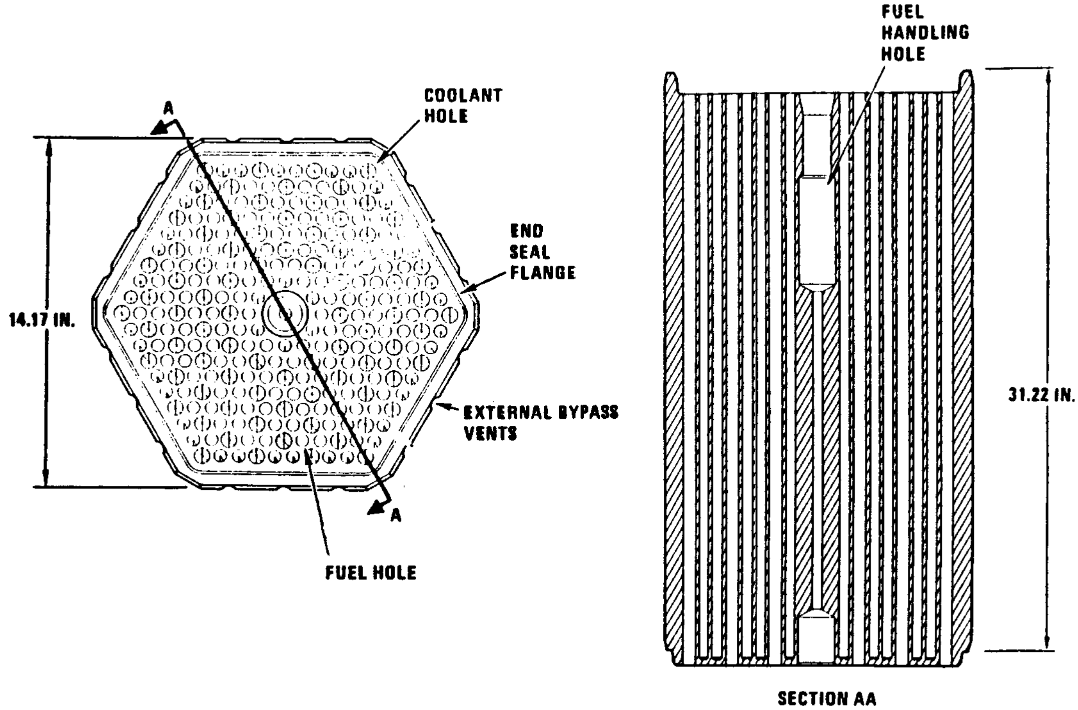

a) STANDARD FUEL ELEMENT

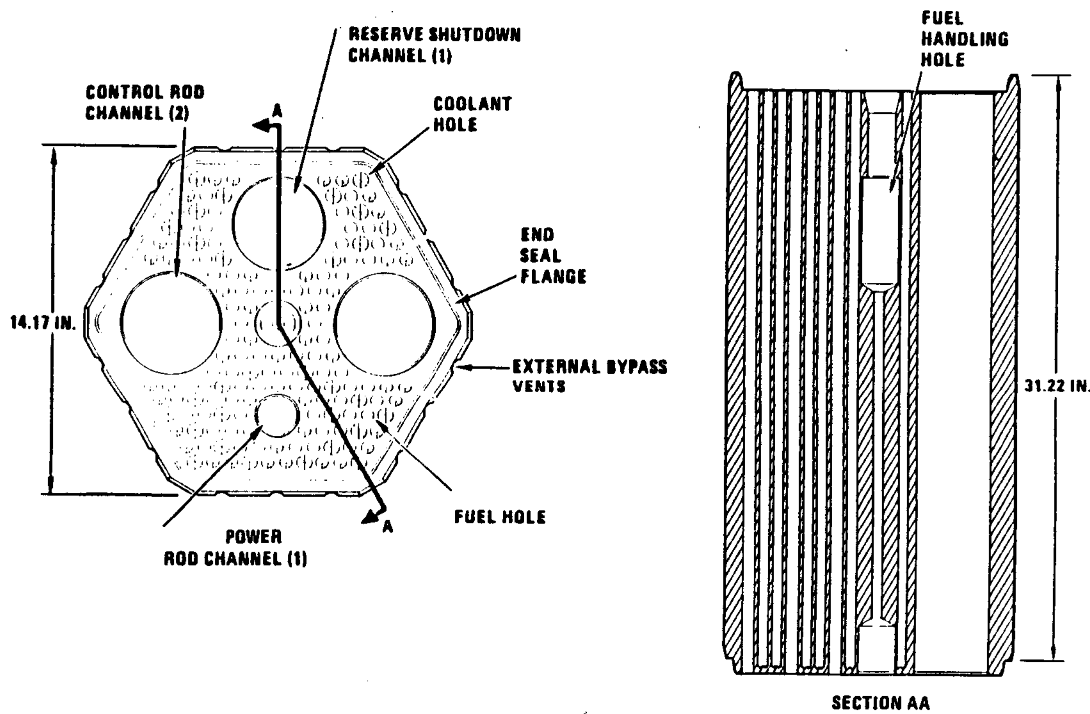

b) CONTROL FUEL ELEMENT

Fig. 2

TWO TYPES OF FUEL ELEMENTS

Figure 3

HTGR PLANT OBJECTIVE AND GOALS

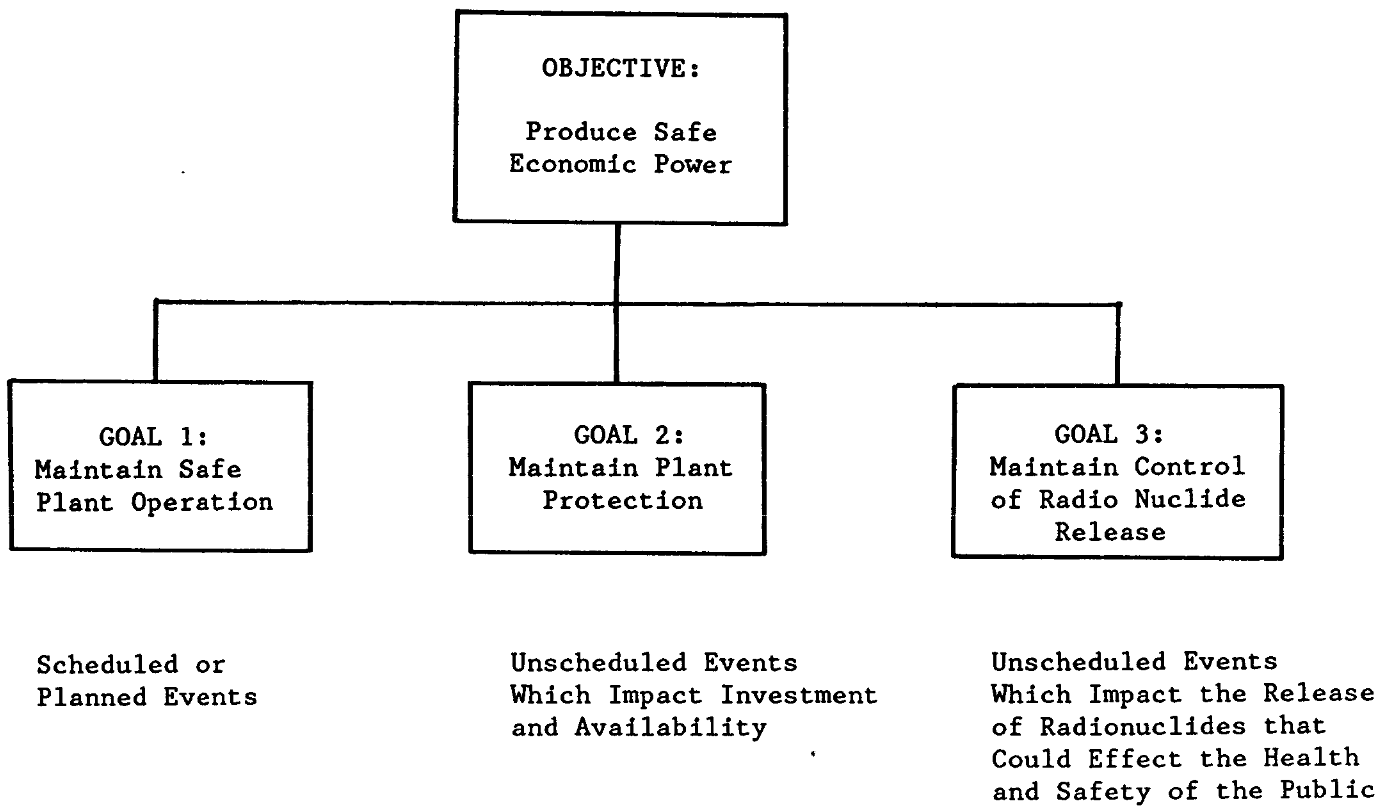

Figure 4

FUEL ELEMENT DESIGN LOOP

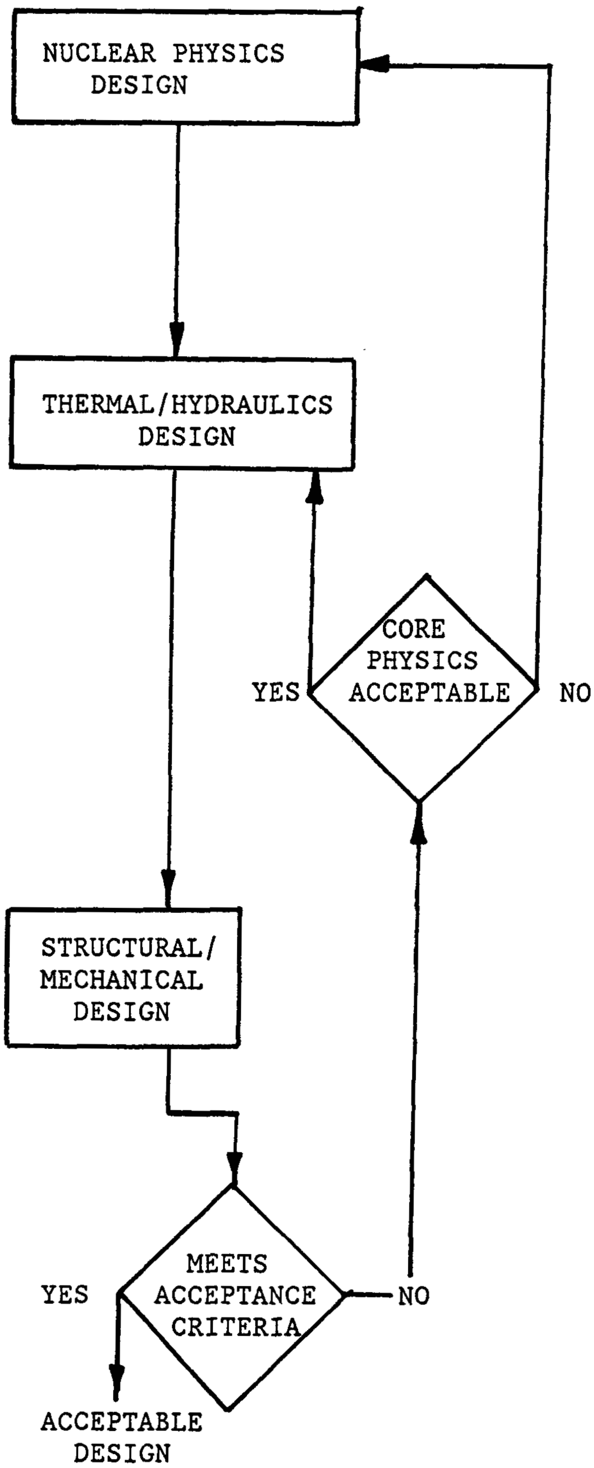

o Total Power Output
o Power Density
o Local Variation of Flux & Power with Time
o Fuel Burnup Schemes
o Control Rod & Burnable Poison Location
o Fuel Rod/Moderator Global Configuration
o Reflector Global Configuration

o System Heat Balance
o Heat Transfer to Primary Coolant
o Fuel Rod Maximum Temperature
o Moderator Global Temperature Field
o Coolant Global Flow Distribution
o Bypass Flow/Temp
o Fuel Rod/Coolant Passage Array Geometry

o Local Flux/Fluence Time History (Interpolation)
o Fuel Element Local Geometry
o Fuel Element Local Temp Time History
o Local Static and Dynamic Loads on Fuel Element
o Local Graphite Material Behavior in Radiation, Temperature and Corrosion Environment
o Calculate Fuel Element Stress Time History and Compare with Structural Criteria

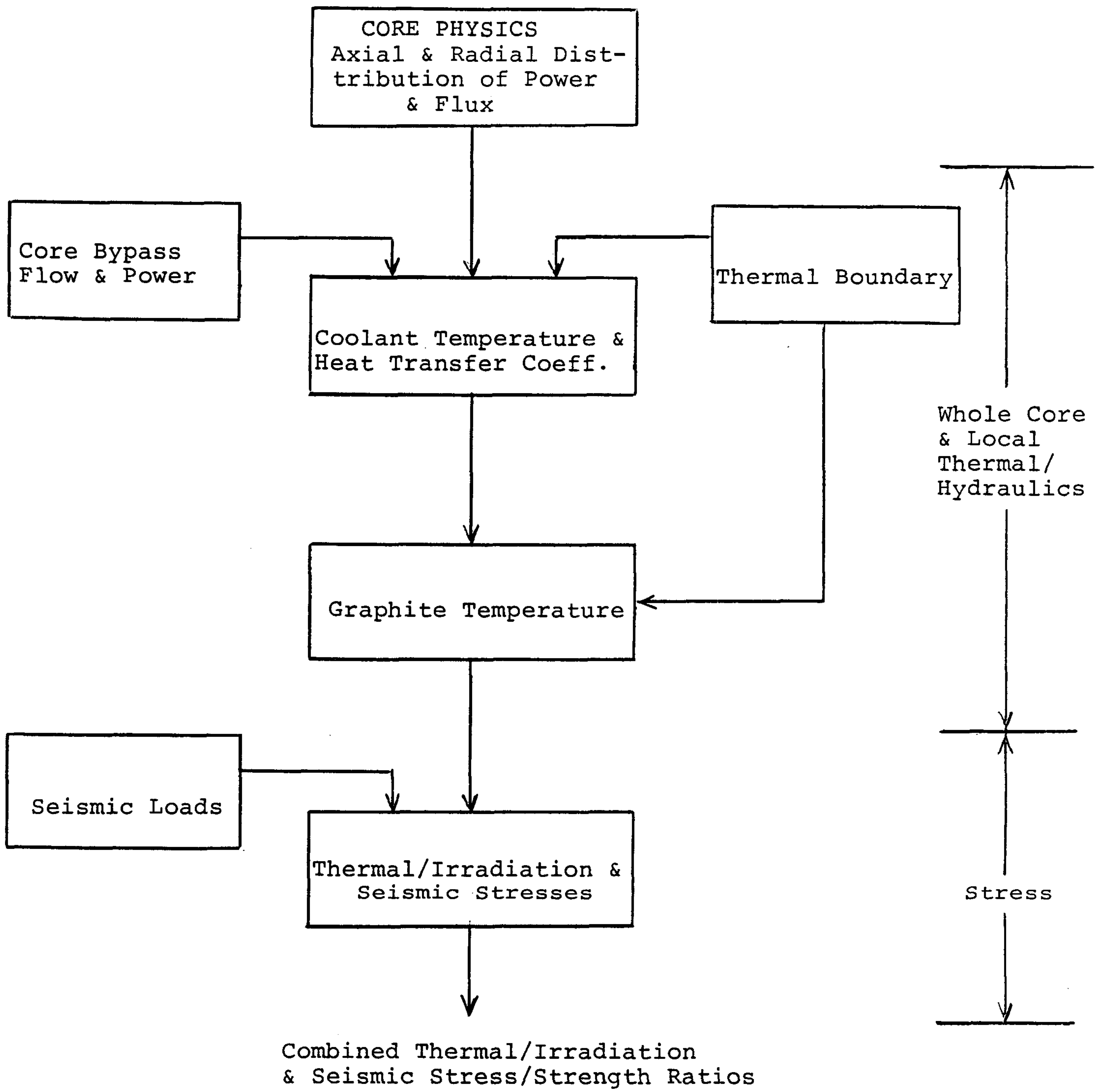

Fig. 5

FUEL ELEMENT ANALYSIS FLOW DIAGRAM

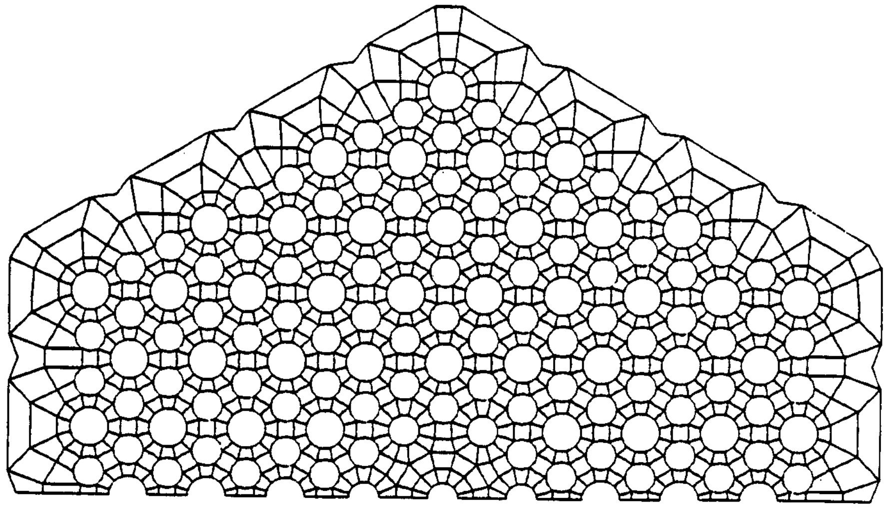

a) STANDARD FUEL ELEMENT

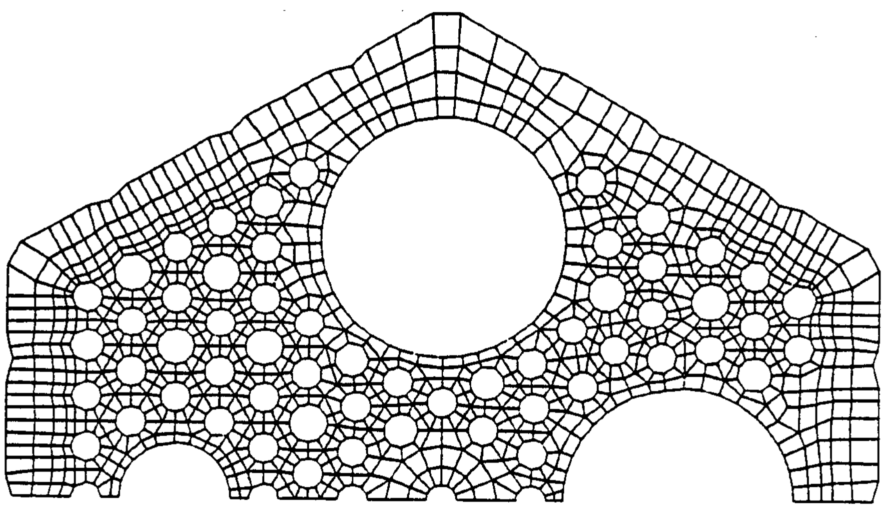

b) CONTROL FUEL ELEMENT

Fig. 6

FINITE ELEMENT MESH FOR
STANDARD AND CONTROL FUEL ELEMENT

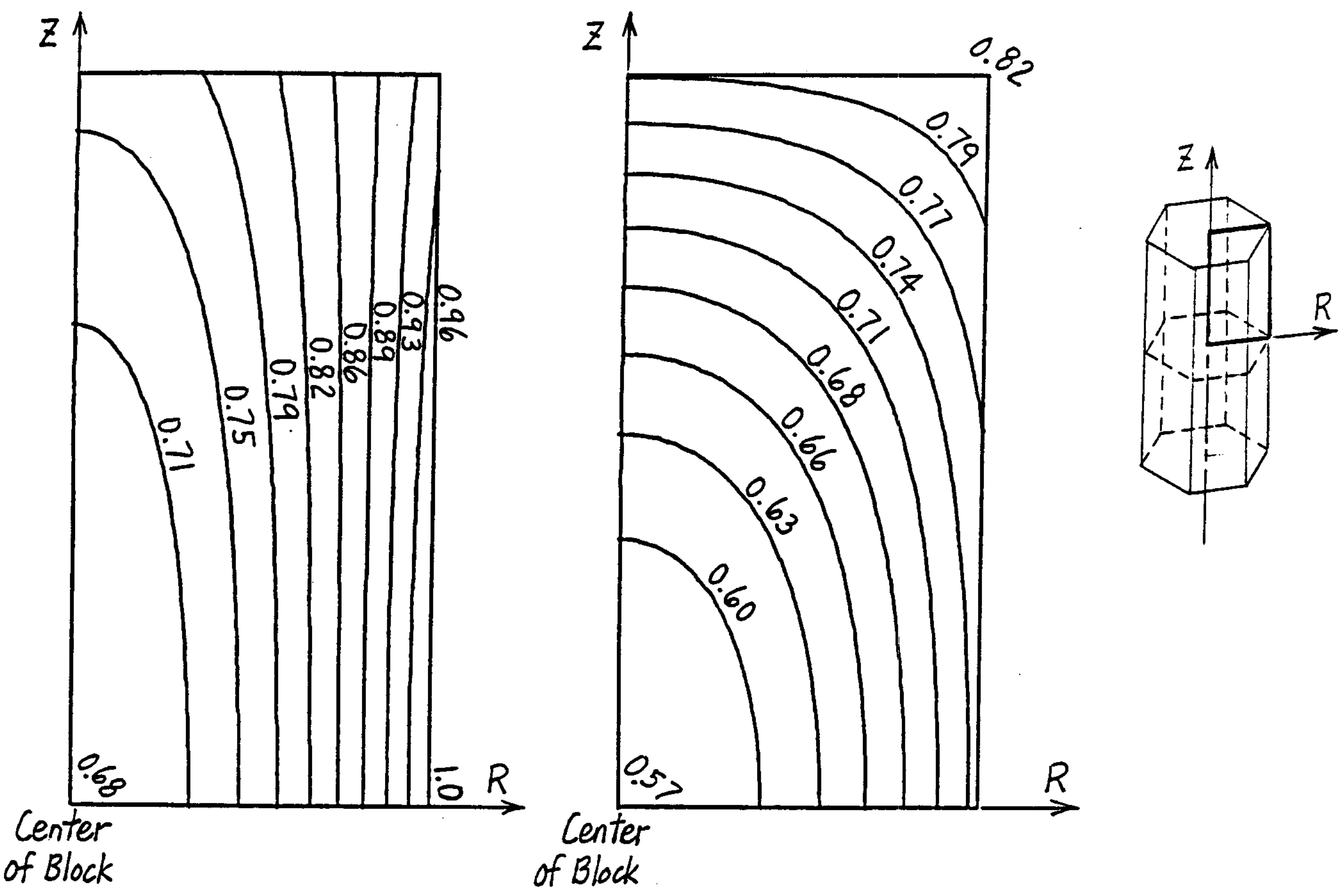

AXIAL STRENGTH DISTRIBUTION

IN-PLATE STRENGTH DISTRIBUTION

Fig. 7

THE STRENGTH DISTRIBUTION WITHIN A FUEL ELEMENT NORMALIZED TO THE MAXIMUM AXIAL STRENGTH (=2755 psi)

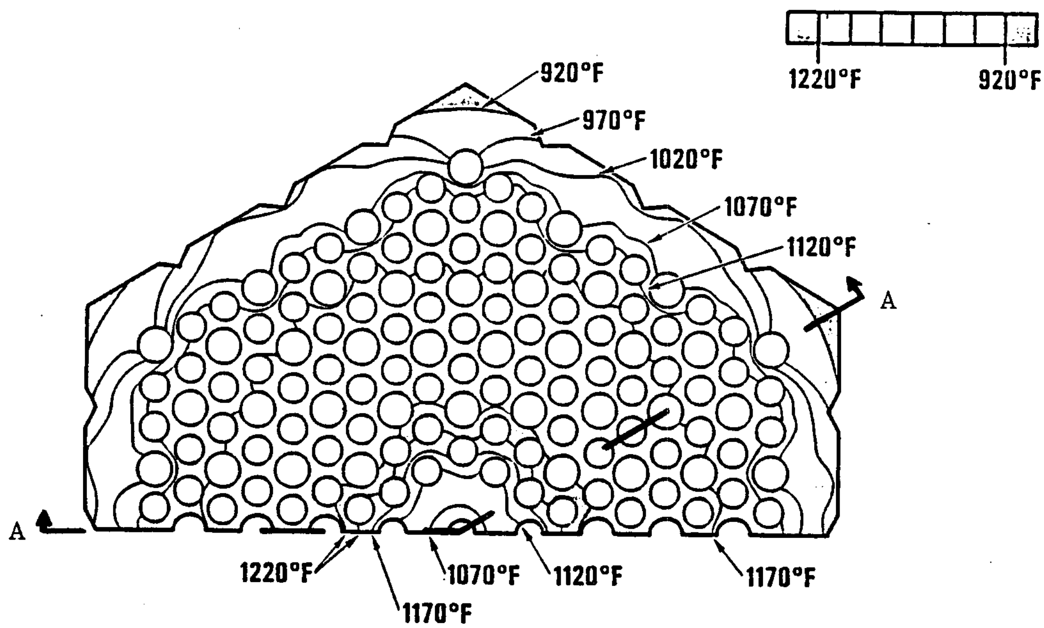

a) TEMPERATURE CONTOURS

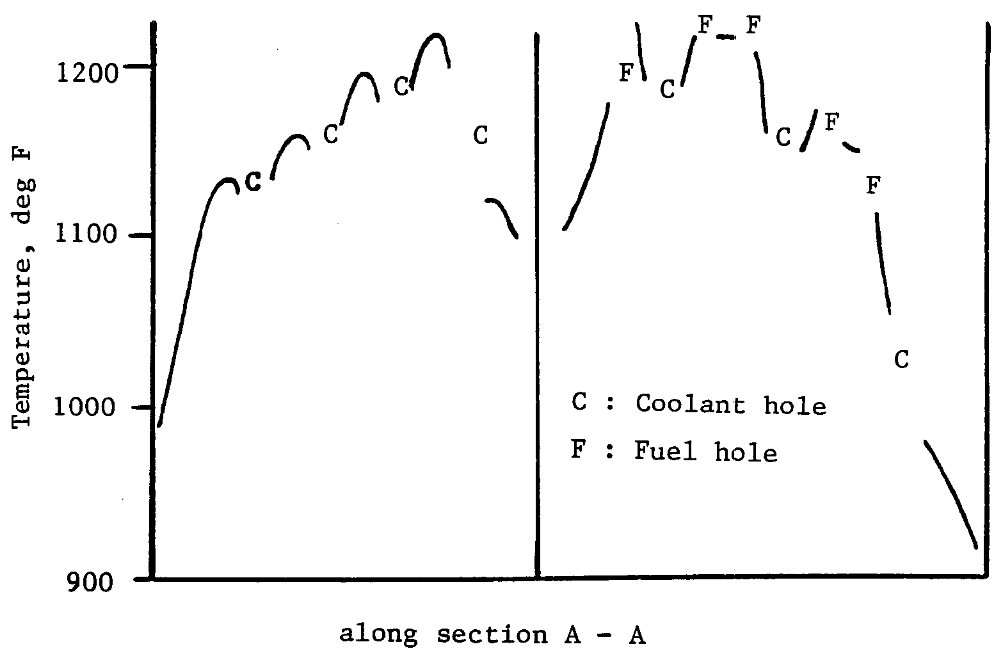

b) DISTRIBUTION ALONG SECTION A - A OF a)

FIG. 8 OPERATING TEMPERATURE AT THE END OF LIFE

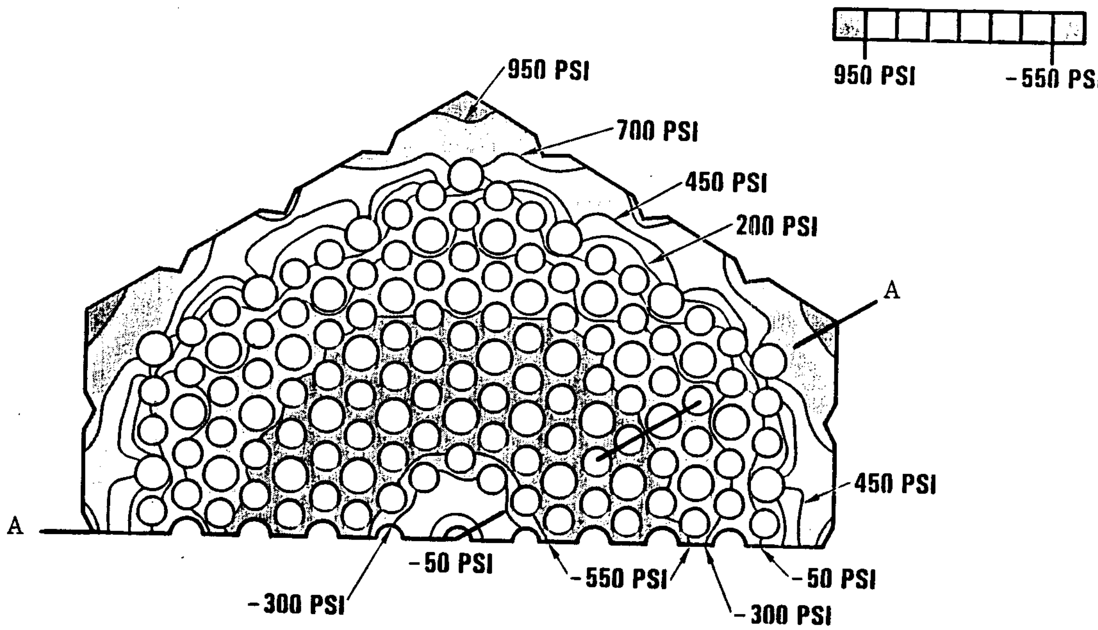

a) STRESS CONTOURS

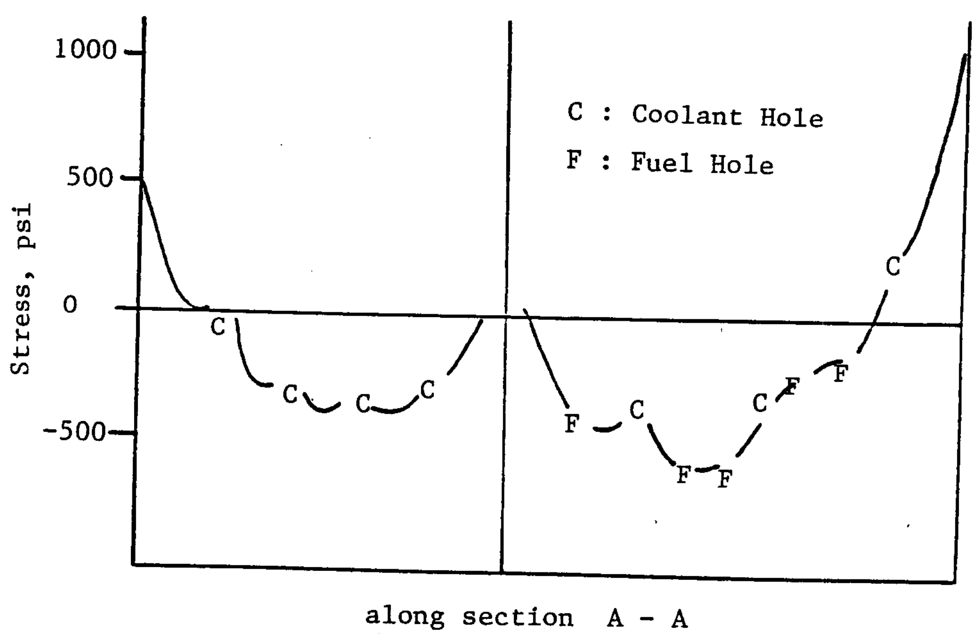

b) DISTRIBUTION ALONG A - A OF a)

FIG. 9 AXIAL OPERATING STRESS AT THE END OF LIFE

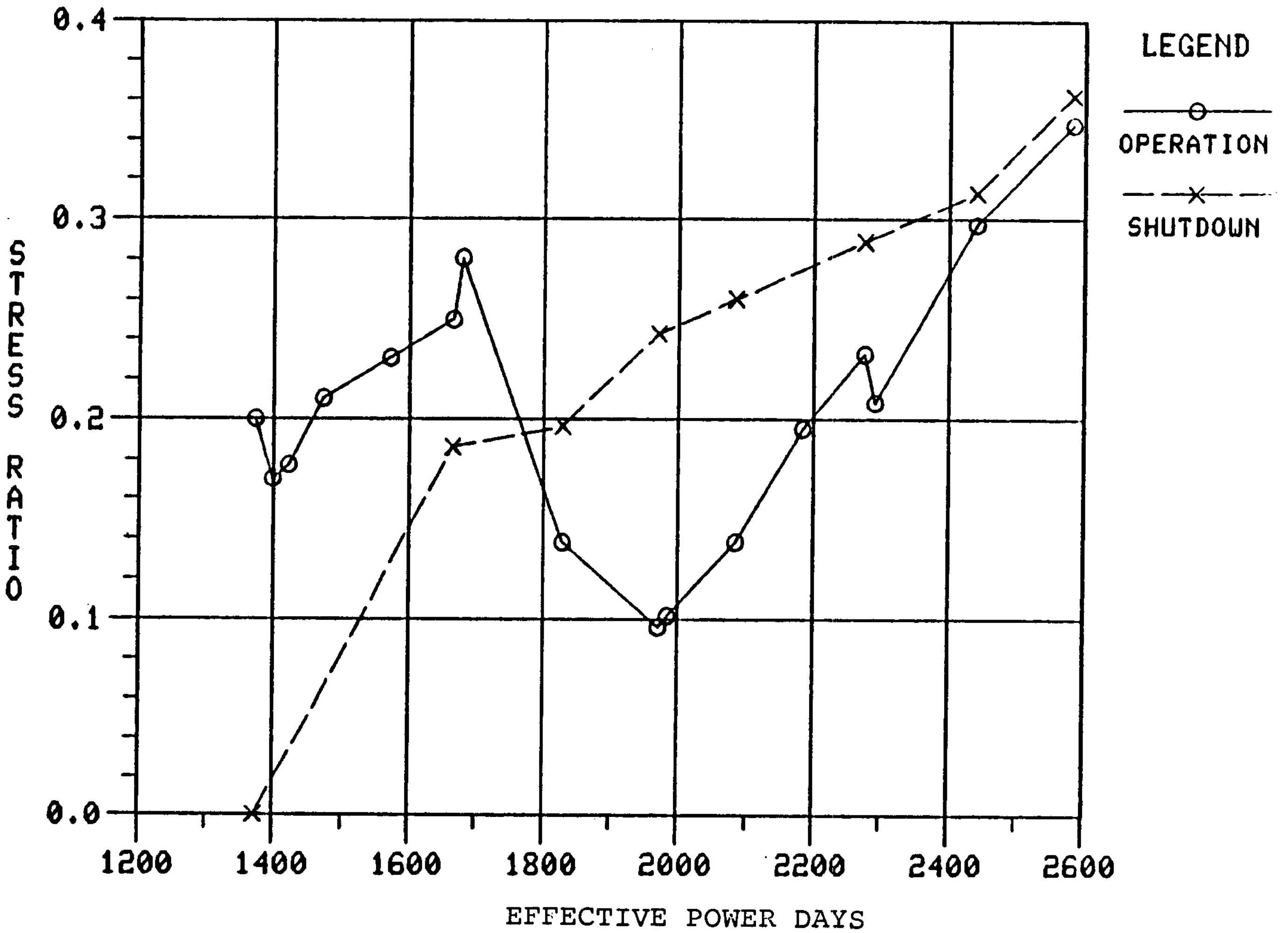

Fig. 10

TYPICAL OPERATING AND SHUTDOWN MAXIMUM STRESS/STRENGTH RATIO HISTORIES IN THE FUEL ELEMENT

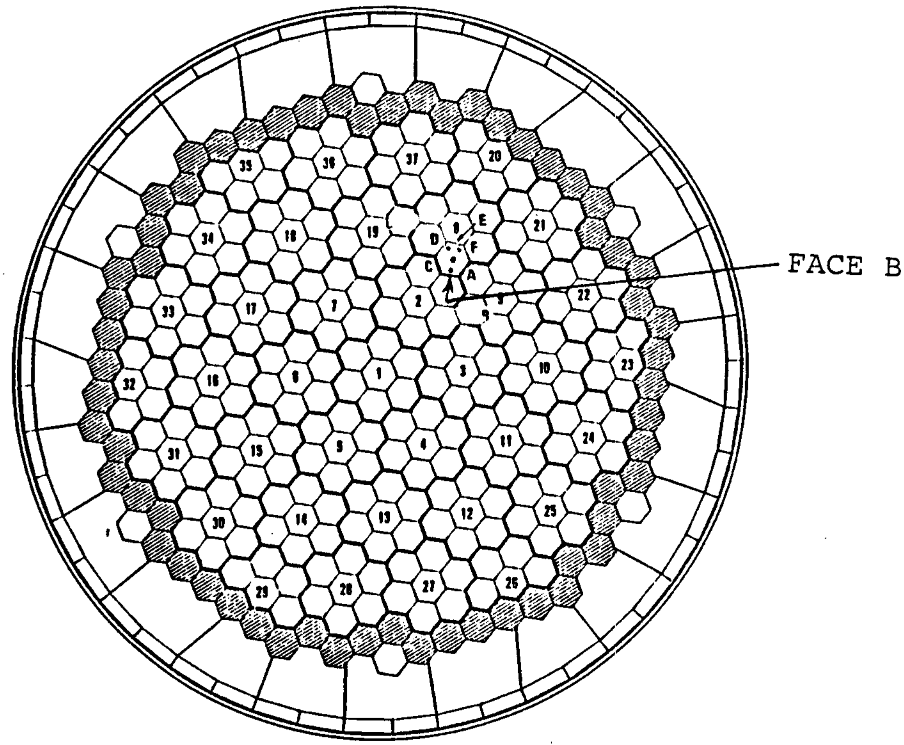

a) LOCATION OF CRACKED BLOCKS IN FSV

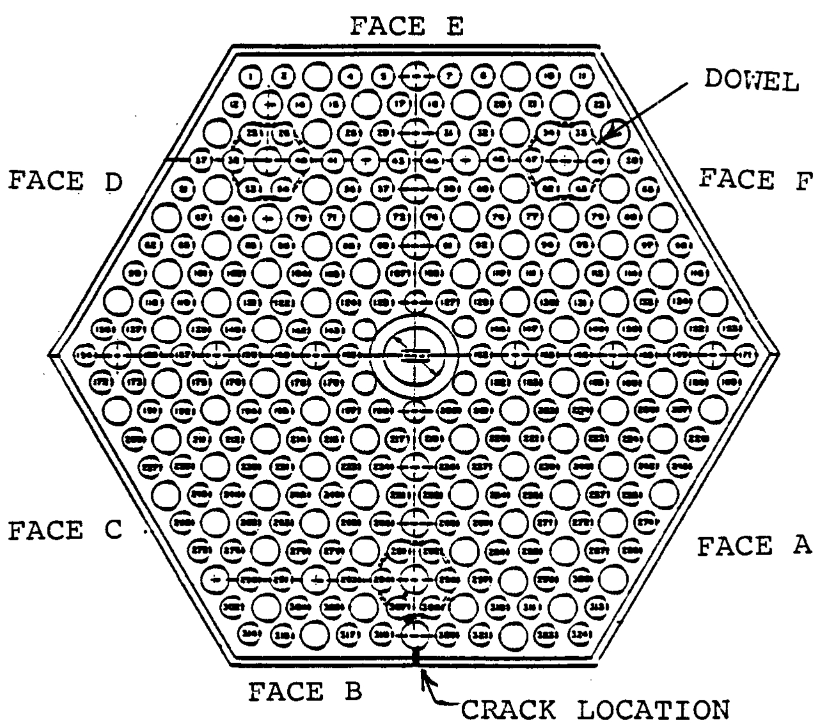

b) BLOCK SHOWING CRACKS

Fig. 11

CRACKED FUEL ELEMENTS IN FSV

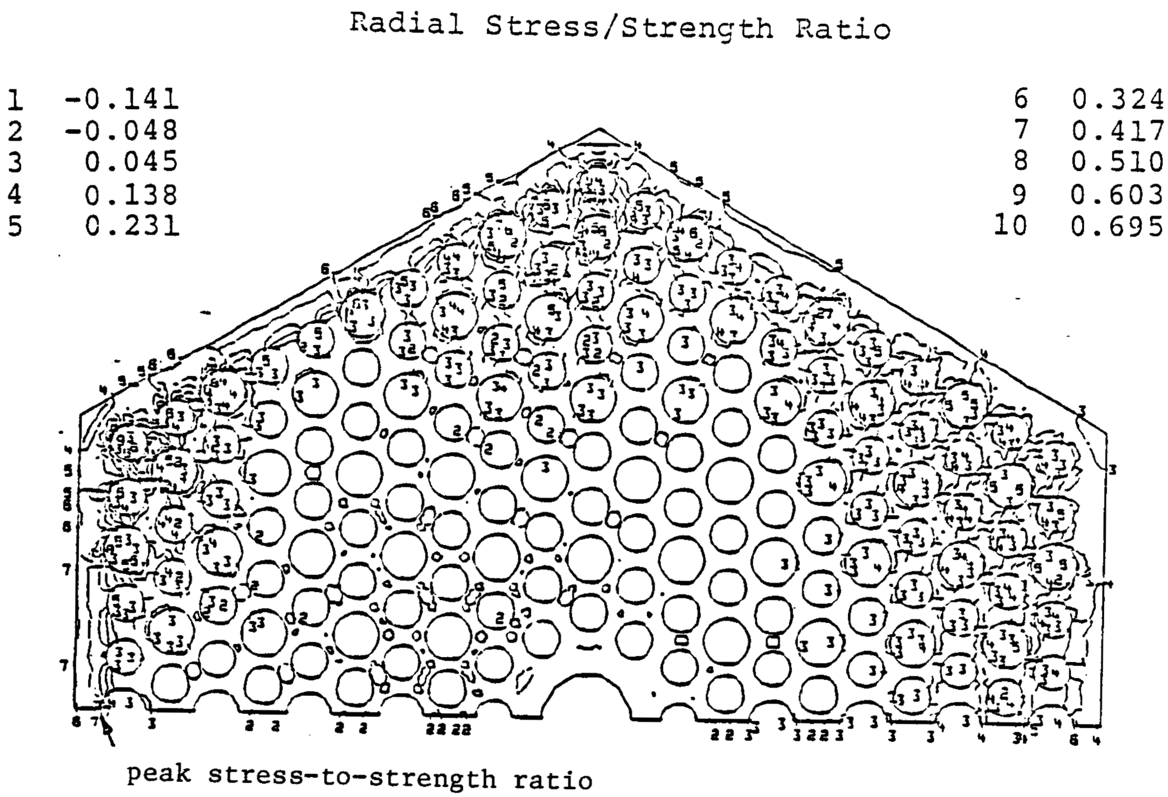

a) LOCATION OF MAXIMUM STRESS-TO-STRENGTH RATIO

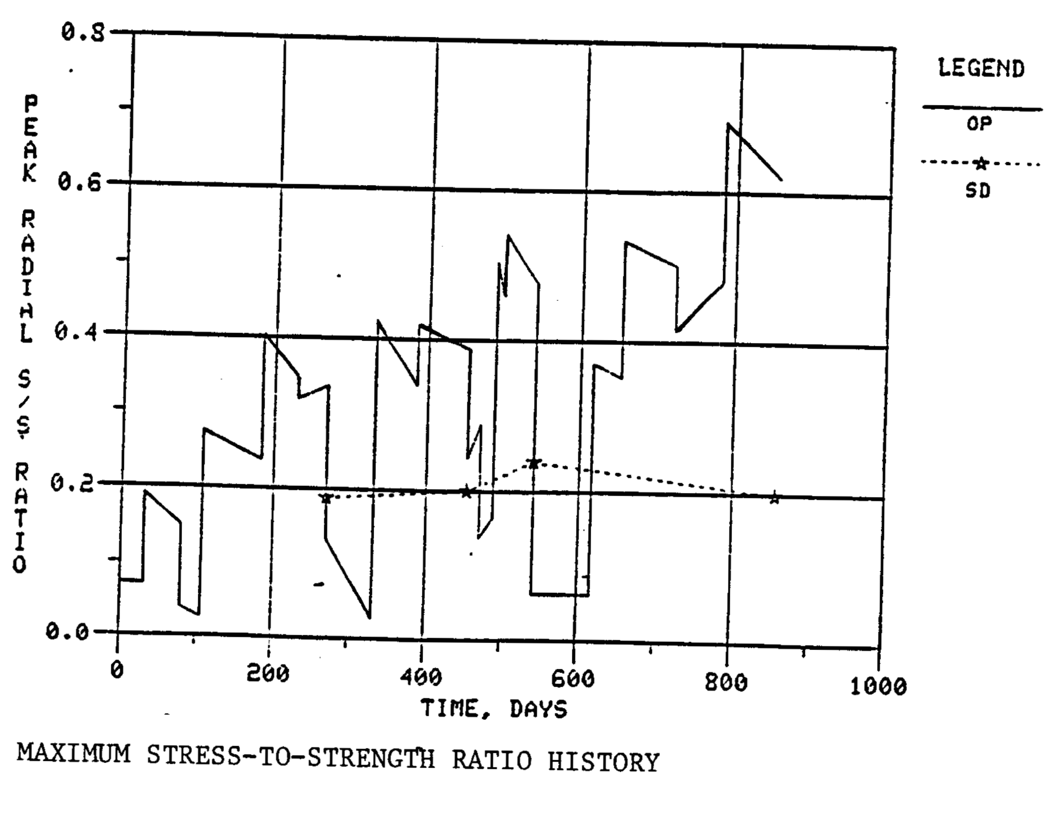

b) MAXIMUM STRESS-TO-STRENGTH RATIO HISTORY

FIG. 12 FSV CRACKED FUEL ELEMENT ANALYSIS

Fig. 13 Stress distribution along symmetry line during crack progression

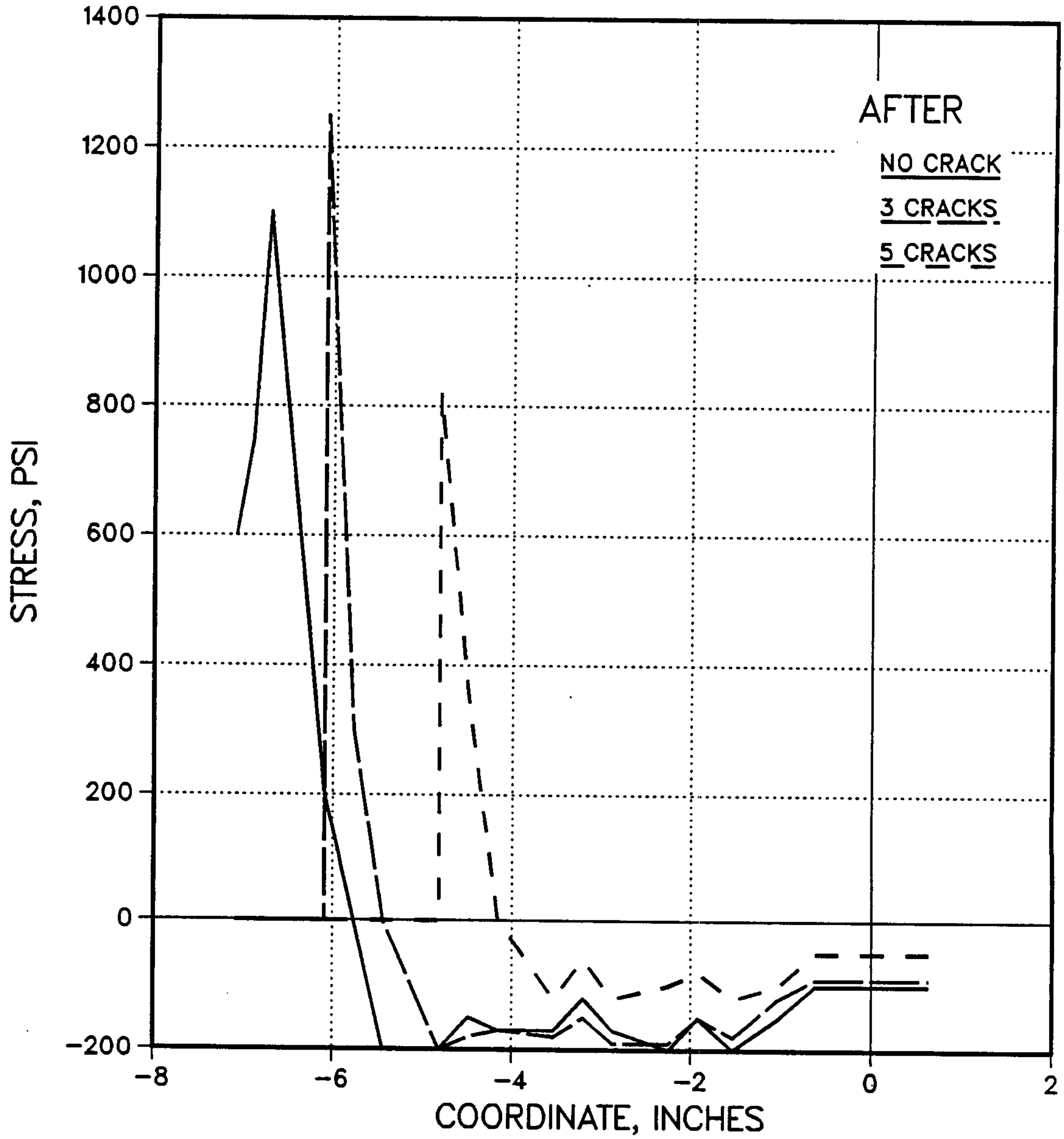

Figure 14

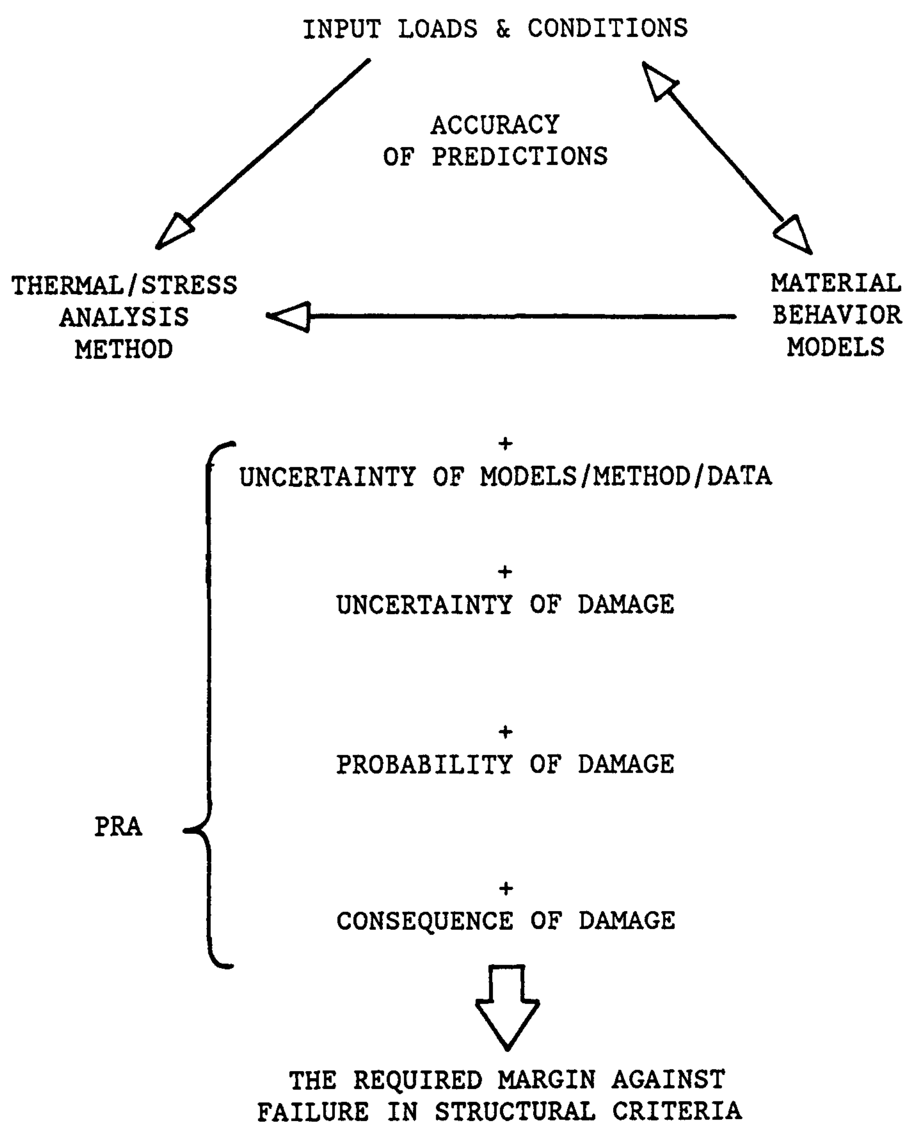
INPUT LOADS & CONDITIONS
ACCURACY
OF PREDICTIONS
THERMAL/STRESS
ANALYSIS
METHOD
MATERIAL
BEHAVIOR
MODELS
+
UNCERTAINTY OF MODELS/METHOD/DATA
+
UNCERTAINTY OF DAMAGE
+
PROBABILITY OF DAMAGE
PRA
+
CONSEQUENCE OF DAMAGE
THE REQUIRED MARGIN AGAINST
FAILURE IN STRUCTURAL CRITERIA

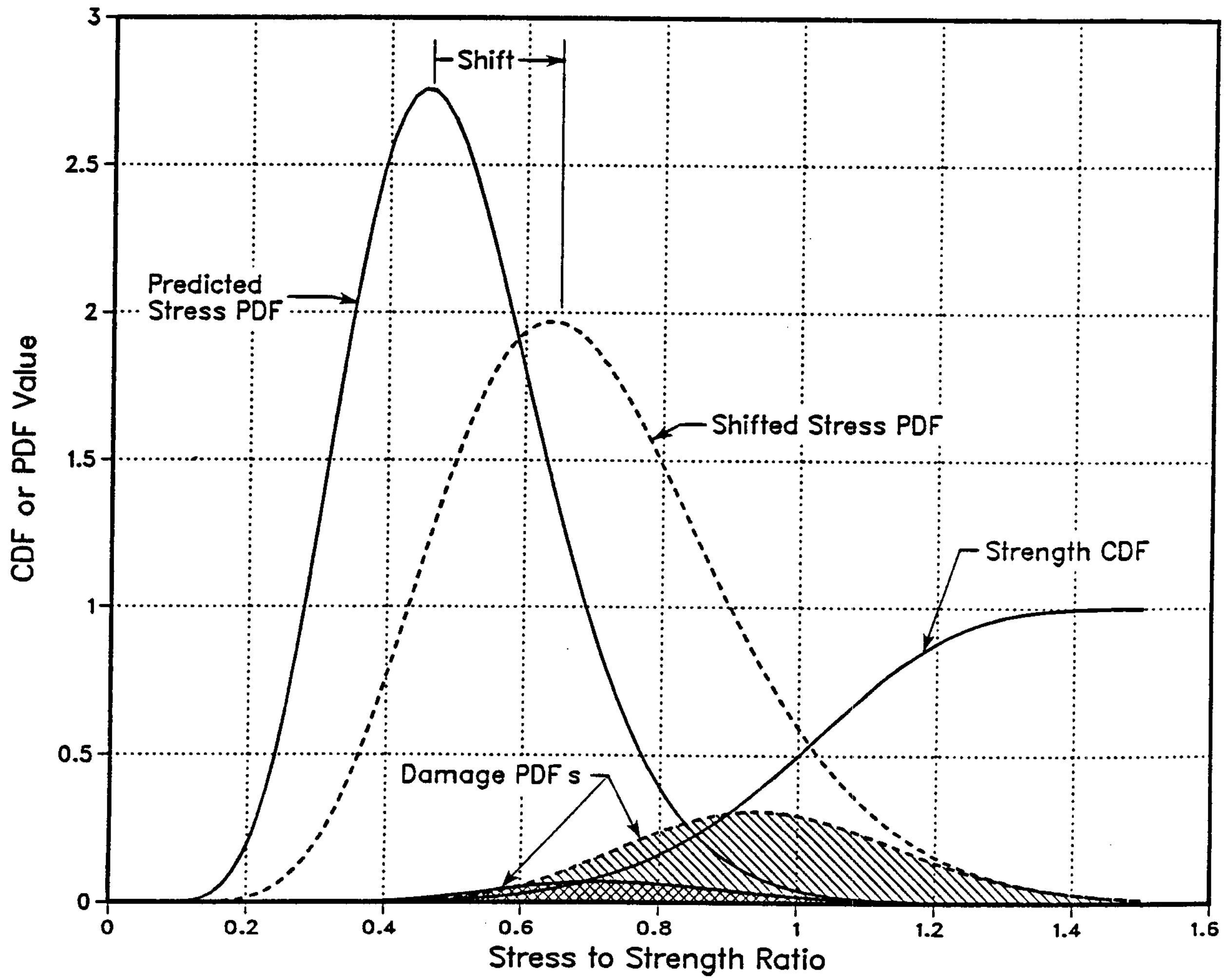

Fig. 15

DAMAGE PROBABILITY CALCULATION